Mesh adaptation for a third-order accurate Euler model

Carabias Alexandre

INRIA, Projet Tropics
2004 route des lucioles - BP 93, 06902 Sophia Antipolis Cedex, France
Alexandre.Carabias@inria.fr

ABSTRACT

1 Introduction

Initially restricted to interpolation errors, *a priori* anisotropic error estimates are available for goal-oriented formulations, and have become an efficient tool for addressing steady Euler flows [5], unsteady Euler flows [3], and more recently steady and unsteady Navier-Stokes ones [**?**]. The error analysis followed the so-called implicit error method, dealing with an invertible system for the deviation between discrete solution and a projection of the continuous one. Estimates were obtained for a second-order mixed-element-volume approximation close to the usual $\mathcal{P}^1$ finite element. Promises given by theory were kept by numerical demonstrators, showing second convergence for shocked flows. The theory also predicts higher-order convergenceExtended-PAPER.tex for the higher-order interpolation of singular flows. For their approximation by a higher-order scheme, anisotropic estimates are needed.

In this paper we consider a central-ENO approximation for the Euler equations. The scheme is third-order accurate on irregular unstructured meshes. The implicit error method is extended to this new context. The resulting *a priori* error analysis is a kind of dual of the *a posteriori* analysis of Barth and Larson [1]. We exploit the principal direction representation of Cao [7]. Then an optimalisation problem for the mesh metric is obtained and analytically solved. For solving the resulting mesh optimality system, we discretise it and apply the global unsteady fixed point algorithm of [3].

The new method is applied to an acoustic propagation benchmark and compared with previous approaches.

2 Numerical approximation

2.1 Model

The 2D Euler equations in a geometrical domain Ω of boundary Γ can be written undExtended-PAPER.texer a nonlinear advection model:

$$\text{Find } u \in \mathcal{V} \text{ such that } \int_{\Omega} v \nabla \cdot \mathcal{F}(u) \, d\,\Omega = \int_{\Gamma} v \mathcal{F}_{\Gamma}(u) \, d\,\Gamma \, \forall \, v \in \mathcal{V}. \tag{1}$$

Here u holds for the conserved unknowns (density, moments components, energy) and $\mathcal{F}$ for the usual Euler fluxes. As right-hand side we have an integral of the various boundary fluxes $\mathcal{F}_\Gamma$ for various boundary conditions, which we do not need to detail here. Defining

$$B(u,v) = \int_\Omega v\nabla \cdot \mathcal{F}(u)\, d\,\Omega$$

and

$$F_u(v) = \int_\Gamma v\mathcal{F}_\Gamma(u)\, d\,\Gamma,$$

this writes:

$$\text{Find } u \in \mathcal{V} \text{ such that } B(u,v) = F_u(v)\; \forall\, v \in \mathcal{V}. \tag{2}$$

We can simplify in a first phase to a linear variant:

$$Extended-PAPER.tex\text{Find } u \in \mathcal{V} \text{ such that } B(u,v) = F(v)\; \forall\, v \in \mathcal{V} \tag{3}$$

in which $B(u,v)$ is bilinear.

2.2 CENO formulation

We choose a reconstruction-based finite-volume method, getting inspired by the unlimited version of the reconstruction technique of Barth [2] and of Central-ENO (CENO) methods developed by Groth and co-workers, [6]. Concerning the location of nodes with respect to mesh elements, we prefer to minimize the number of unknowns with respect to a given mesh and therefore we keep the vertex-centered location already successfully used for second-order anisotropic (Hessian-based or Goal-oriented) mesh adaptation. The considered numerical approximation is described in [8]. Its main features are: (a) vertex centered, (b) dual median cells around the vertex, (c) a single mean square conservative quadratic reconstruction for each dual cell (d) HLLC Riemann solver for fluxes integration, (e) explicit multi-stage time-stepping.

The computational domain is divided in triangles and in a dual tesselation in cells, each cell C_i being built around a vertex i, with limits following sections of triangle medians.

We define the discrete space $\mathcal{V}_0$ of functions that are constant on any dual cell C_i.

For an advection model written (3), the discrete CENO version writes:

$$\text{Find } u_0 \in \mathcal{V}_0 \text{ such that } B(R_2^0 u_0, v_0) = F(v_0)\; \forall\, v_0 \in \mathcal{V}_0$$

We observe that this produces a finite volume formulation:

$$\forall C_i, \quad \int \nabla \cdot \mathcal{F}(R_2^0 u_0)\, d\,\Omega = \int_{\partial C_i \cap \Gamma} \mathcal{F}_\Gamma(R_2^0 u_0)\, d\,\Gamma$$

or:

$$\forall C_i, \quad \int_{\partial C_i} \mathcal{F}(R_2^0 u_0) \cdot \mathbf{n}\, d\,\Gamma - \int_{\partial C_i \cap \Gamma} \mathcal{F}_\Gamma(R_2^0 u_0)\, d\,\Gamma = 0. \tag{4}$$

It remains to define R_2^0. It is a reconstruction operator which reconstructs a function of $\mathcal{V}_0$ in each cell C_i under the form of a second-order polynomial:

$$R_2^0 u_0 | C_i = \mathcal{P}_2(x,y).$$

According to the ENO principle, a mean square formula is applied from the dual cell averages around the considered dual cell. The knowledge of this reconstruction does not completely define the above approximation. Indeed, the reconstruction performed in each cell is generally discontinuous at interfaces. In order to fix an integration value at the interface, we can consider an arithmetic mean of the fluxes values for the two reconstruction values:

$$\mathcal{F}(R_2^0 u_0)^*|_{\partial C_i \cap \partial C_j} \cdot \mathbf{n} = \frac{1}{2} \left(\mathcal{F}(R_2^0 u_0)|_{\partial C_i} + \mathcal{F}(R_2^0 u_0)|_{\partial C_j} \right) \cdot \mathbf{n} \tag{5}$$

where $(R_2^0 u_0)|_{\partial C_i}$ holds for the value at cell boundary of the reconstructed $R_2^0 u_0|_{C_i}$ on cell C_i. This formulation produces a central-differenced numerical approximation which is third order accurate, but it cannot be used as it is in nonlinear applications, due to a lack of stability.

2.3 Vertex-centered low dissipation CENO2

Scheme (4) is usually combined with an approximate Riemann solver used instead of (5). This latter option produces a rather dissipative third-order accurate scheme. Now we are here interested only by rather mild non-linear effects. Scheme (4)(5) is then stabilised as in [9], *i.e* completed by two extra terms: the first term compensate partially the main dispersive error. The second one introduces a six-th order dissipation. We refer to [9] for details and for numerical experiments showing the interest of this new CENO2 variant.

3 Error analysis

We drive an *a priori* analysis which is the dual of the *a posteriori* analysis proposed in [1]. Let be $M(u)$ the scalar output we want accurately compute. We shall concentrate the error reduction effort on the following expression:

$$\delta M = M(R_2^0 \pi_0 u - R_2^0 u_0).$$

The adjoint state $u_0^* \in \mathcal{V}_0$ is the solution of:

$$\frac{\partial B}{\partial u}(R_2^0 u_0)(R_2^0 v_0, u_0^*) = M(R_2^0 v_0), \ \forall \ v_0 \in \mathcal{V}_0.$$

We also need to define the projection π_0:

$$\pi_0 : (V) \rightarrow (V_0),$$

$$v \mapsto \pi_0 v$$

$$\forall \ C_i, \text{dual cell}, \pi_0 v|_{C_i} = \int_{C_i} v dx.$$

Then we can write, successively:

$$
\begin{aligned}
M(R_2^0 \pi_0 u - R_2^0 u_0) &= \frac{\partial B}{\partial u}(R_2^0 u_0)(R_2^0 \pi_0 u - R_2^0 u_0, u_0^*) & \text{(adjoint eq.)} \\
&\approx B(R_2^0 \pi_0 u, u_0^*) - B(R_2^0 u_0, u_0^*) \\
&\approx B(R_2^0 \pi_0 u, u_0^*) - F(u_0^*) & \text{(disc.state eq.)} \quad (6) \\
&\approx B(R_2^0 \pi_0 u, u_0^*) - B(u, u_0^*) & \text{(cont.state eq.)} \\
&\approx \frac{\partial B}{\partial u}(u)(R_2^0 \pi_0 u - u, u_0^*)
\end{aligned}
$$

In the case of Euler equations, we have:

$$\frac{\partial B}{\partial u}(u)(R_2^0 \pi_0 u - u, u_0^*) \approx \sum_i \int_{C_i} u_0^* \nabla \cdot \mathcal{F}'(u)(R_2^0 \pi_0 u - u) dx$$

where the sum applies for all dual cell C_i of the mesh. Noting that u_0 is constant over each cell C_i, we can transform the above with an integration by parts:

$$B(R_2^0 \pi_0 u - u, u_0^*) \approx - \sum_i \int_{\partial C_i} u_0^* \mathcal{F}'(R_2^0 \pi_0 u - u) \cdot \mathbf{n} \, d\sigma.$$

Observing that two integrals are computed on each interface C_{ij} separating two neighboring cells:

$$B(R_2^0 \pi_0 u - u, u_0^*) \approx - \sum_{C_{ij}} \int_{\partial C_i \cap \partial C_j} \left[\left(u_0^* \mathcal{F}'(R_2^0 \pi_0 u - u) \right)_{C_i} - \left(u_0^* \mathcal{F}'(R_2^0 \pi_0 u - u) \right)_{C_j} \right] \cdot \mathbf{n} \, d\sigma.$$

Even for $u_0^* \approx \pi_0 u^*$, with u^* smooth, the discontinuity at interface of u_0^* is of order 1. By construction of the higher order reconstruction, the discontinuity at interface of $R_2^0 \pi_0 u - u$ is of higher order. Then:

$$\left(u_0^* \mathcal{F}'(R_2^0 \pi_0 u - u) \right)_{C_i} - \left(u_0^* \mathcal{F}'(R_2^0 \pi_0 u - u) \right)_{C_j} \approx$$
$$\frac{1}{2} \left[(u_0^*)_{C_i} - (u_0^*)_{C_j} \right] \left[\left(\mathcal{F}'(R_2^0 \pi_0 u - u) \right)_{C_i} + \left(\mathcal{F}'(R_2^0 \pi_0 u - u) \right)_{C_j} \right]$$

We shall show that $R_2^0 \pi_0 u - u$ can be replaced by a smooth function of the local third derivatives and local mesh size:

$$R_2^0 \pi_0 u - u \approx G(u^{(3)}, (\delta \mathbf{x})^3).$$
$$\mathcal{F}'(R_2^0 \pi_0 u - u) \approx \mathcal{F}'(G(u^{(3)}, (\delta \mathbf{x})^3)).$$

On the other side, the jump term $u_0^*|_{C_i} - u_0^*|_{C_j}$ is a first derivative of u^* times the distance between the centroids of the two cells, or equivalently (at first-order) the vertices i and j. The integration of this term over the section of interface $\partial C_i \cap \partial C_j$ is essentially the (double of the) area of the four triangles delimited by i, j and the centroids of triangles havin ij as common side. The set of all these triangles is a tessellation of the computationa domain. Then:

$$|B(R_2^0 \pi_0 u - u, u_0^*)| \approx \leq 2 \int_\Omega K(u, u^*) |G(u^{(3)}, (\delta \mathbf{x})^3)| \, d\Omega$$

with

$$K(u, u^*) = |(\mathcal{F}')^*| |\nabla u^*|.$$

Optimal metric

The parametrization of the mesh is a Riemannian metric defined in each point $\mathbf{x}$ of the computational domain by a symmetric matrix, $\mathcal{M}(\mathbf{x}) = \mathcal{R}(\mathbf{x}) \Lambda(\mathbf{x}) \mathcal{R}^t(\mathbf{x})$.

$\mathcal{R} = (\mathbf{e}_\xi, \mathbf{e}_\eta)$, the rotation matrix built with the normalised eigenvectors of $\mathcal{M}$, parametrises the two orthogonal stretching directions of the metric.

Λ is a 2×2 diagonal matrix with eigenvalues $\lambda_1 = (m_\xi)^{-2}$ and $\lambda_2 = (m_\eta)^{-2}$ where m_ξ and m_η represent the two directional local mesh sizes in the characteristic/stretching directions of $\mathcal{M}$.

Given a metric or -somewhat equivalently- a mesh described by it, we modelise the quadratic interpolation error as follows:

$$|u(\mathbf{x}) - \mathcal{P}_2 u(\mathbf{x})| = |\frac{\partial^3 u}{\partial \tau^3}|(\delta\tau)^3 + |\frac{\partial^3 u}{\partial n^3}|(\delta n)^3 \ .$$

After the *a priori* analysis, we have to minimise the following error:

$$\mathcal{E} = \int K(u, u^*) \left(|\frac{\partial^3 u}{\partial n^3}|(\delta n)^3 + |\frac{\partial^3 u}{\partial t^3}|(\delta t)^3 \right) \ dx dy.$$

We proceed as for the second-order metric analysis, e.g. [5] and we get :

$$\mathcal{M}_{opt} = d_{opt} \mathcal{R}^t \begin{pmatrix} e_{opt}^{-1} & 0 \\ 0 & e_{opt} \end{pmatrix} \mathcal{R}$$

with

$$d_{opt} = \frac{N}{C} \left(|K(u, u^*) u_{\xi\xi\xi}| e^{\frac{3}{2}} + |K(u, u^*) u_{\eta\eta\eta}| e^{-\frac{3}{2}} \right)^{\frac{2}{5}},$$
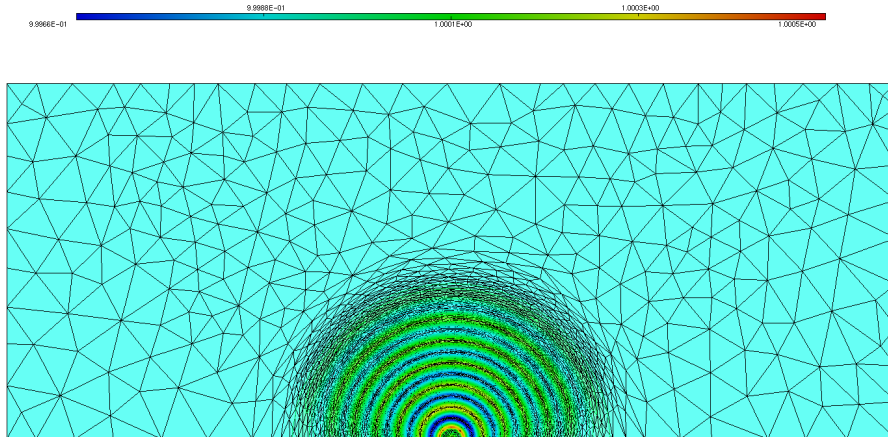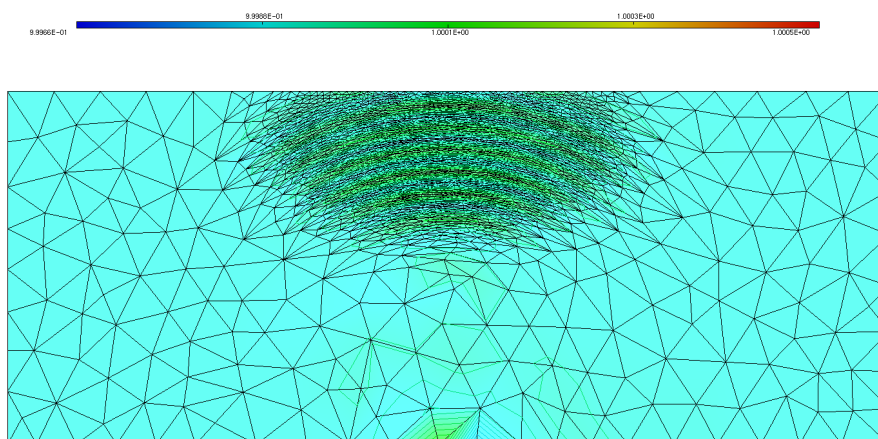
with

$$e_{opt} = \frac{m_\xi}{m_\eta} = \left(\frac{|u_{\eta\eta\eta}| + \varepsilon}{|u_{\xi\xi\xi}| + \varepsilon} \right)^{\frac{1}{3}},$$

and with

$$C = \int \left(|K(u, u^*) u_{\xi\xi\xi}| e^{\frac{3}{2}} + |K(u, u^*) u_{\eta\eta\eta}| e^{-\frac{3}{2}} \right)^{\frac{2}{5}} \ dx dy.$$

Preliminaries Results

References

[1] T.J. Barth and M.G. Larson. A-posteriori error estimation for higher order Godunov finite volume methods on unstructured meshes. In Herbin and Kroner, editors, Finite Volumes for Complex Applications III, pages 4163. Hermes Science Pub., London, 2002.

[2] T.J. Barth, "Recent developements of high-order k-exact reconstruction on unstructured meshes", AIAA Paper 93-0668, 1993.

[3] A. Belme, A. Dervieux and F. Alauzet, Goal-oriented anisotropic mesh adaptation for unsteady flows, Proceeding ECCOMAS CFD Conference, Lisbon, june 2010.

[4] O.C. Zienkiewicz and J.Z. Zhu, The superconvergent patch recovery and a posteriori error estimates. Part 1: The recovery technique, I.J. Num. Meth. Eng., 33:7,1331-1364,1992.

[5] A. Loseille, A. Dervieux, P.J. Frey and F. Alauzet, "Achievement of global second-order mesh convergence for discontinuous flows with adapted unstructured meshes", AIAA paper 2007-4186, Miami, FL, USA, June 2007.

[6] L. Ivan and C. P. T. Groth, High-Order Central ENO Finite-Volume Scheme with Adaptive Mesh Refinement , AIAA Paper 2007-4323, June 2007.

[7] Weiming Cao, An interpolation error estimate on anisotropic meshes in R^n and optimal metrics for mesh refinement. *SIAM J. Numer. Anal.* 45 (2007), no. 6, 23682391.

[8] H. Ouvrard, T. Kozubskaya, I. Abalakin, B. Koobus, and A. Dervieux, Advective vertex-centered recon- struction scheme on unstructured meshes. INRIA Research Report, RR-7033 (2009).

[9] A. Carabias , O. Allain, A. Dervieux. Dissipation and dispersion control of a quadratic-reconstruction advection scheme, European Workshop on High Order Nonlinear Numerical Methods for Evolutionary PDEs: Theory and Applications, Trento, Italy, april 11-15, 2011.